

Time Evolution of the Magnetic Structure of a Field-Reversed Configuration in a Super-Alfvénic Translation Process^{*)}

Tomohiko ASAI, Shunsuke AKAGAWA, Kazuhiro AKIMOTO, Naoki TADA,
Tutomu TAKAHASHI and Hiroyasu TAZAWA

Nihon University, 1-8-14 Kanda-Surugadai, Chiyoda-ku, Tokyo 101-8308, Japan

(Received 7 December 2010 / Accepted 9 May 2011)

The effects of the conducting wall on the FRC translation process have been investigated by using a confinement coil with a toroidal cut on the coil spool. Using the simple ring current model, the induced current on the conducting coil spool and chamber wall, and the separatrix shape, were estimated. A deceleration force produced by the induced currents equals to approximately 10% of the acceleration one generated by the gradient of the magnetic guide field. To investigate these effects experimentally, FRC translation was performed with a toroidal cut on the coil spool. In this case, typical translation velocity was increased from 100 to 150 km/s. However, a shift type (toroidal mode number $n = 1$) motion was triggered, likely by the asymmetry of the wall boundary.

© 2011 The Japan Society of Plasma Science and Nuclear Fusion Research

Keywords: field-reversed configuration (FRC), super-Alfvénic translation, separatrix shape, rotational mode instability, shift motion

DOI: 10.1585/pfr.6.2402151

1. Introduction

A field-reversed configuration (FRC) plasma is a compact toroid with no significant toroidal magnetic field. This plasma has unique advantages as a fusion reactor core, for example, a simple geometry, an extremely high beta value ($\sim 100\%$) and an open magnetic field region as a natural divertor. Due to the above unique potential, FRC plasma has been attracting attention as an advanced fuel (D-³He) fusion reactor core.

In the FRC, a centrifugally driven interchange instability with toroidal mode number $n = 2$ is the most serious global instability limiting the configuration lifetime. However, translation experiments in the FRC Injection Experiments (FIX) and the Translation Confinement and Sustainment Experiment (TCS) have shown improved stability and confinement after a process of super-Alfvénic translation [1]. The super-Alfvénic merging of two FRCs at the C-2 facility has also shown improved confinement properties in FRC [2]. Super-Alfvénic translation has been recently initiated on the flexible theta-pinch based FRC device, NUCTE (Nihon University Compact Torus Experiment). In this series of experiments, delayed onset-time of the rotational instability and improved flux confinement have also been observed. These phenomena have been discussed as the effects of the background neutral particle and weakly ionized plasma injected into the translated FRC [3, 4].

The unique feature of NUCTE is the conducting chamber walls in both the upstream and downstream mir-

ror regions. The metallic chamber potentially provides an additional deceleration force on the plasma and reduces the interaction between the metallic surface and the plasma [4]. In this study, a time evolution of the magnetic structure in the translation process was investigated, to reveal the mechanism of the improved confinement of translated FRC plasma. Also, the FRC plasma was simulated as a set of several ring currents. Then the inductive currents induced on the confinement coil spool and metallic chamber were estimated. Analysis revealed an inductive current of 15-25 kA induced on the spool and the chamber wall, which affected on the translated FRC plasma. To verify this effect experimentally, the global behavior of the FRC was observed using coil spools with a toroidal cut.

2. Experimental Apparatus and Diagnostic

The arrangement of the NUCTE-III/T device for this study is shown in Fig. 1 (a). A FRC plasma is formed by a field-reversed theta-pinch (FRTP) method and translated along the gradient of the guide field. The tapered theta-pinch coil of 1.3 m in length consists of coil elements with diameters of 0.36, 0.34, 0.32 and 0.30 m. A working gas of deuterium is puffed into the middle of the transparent quartz discharge tube by a fast gas-puff valve. The equivalent gas pressure is approximately 10 mTorr for the static gas-fill method. Pre-ionized plasma is formed by a theta-ionization method in the formation chamber, with a typical bias field strength of 32 mT. Then, the main compression field, with a raising time of 3 μ s, a peak strength of 0.7 T, and a decay time of 120 μ s, is applied, in order to generate a FRC.

author's e-mail: asai.tomohiko@nihon-u.ac.jp

^{*)} This article is based on the presentation at the 20th International Toki Conference (ITC20).

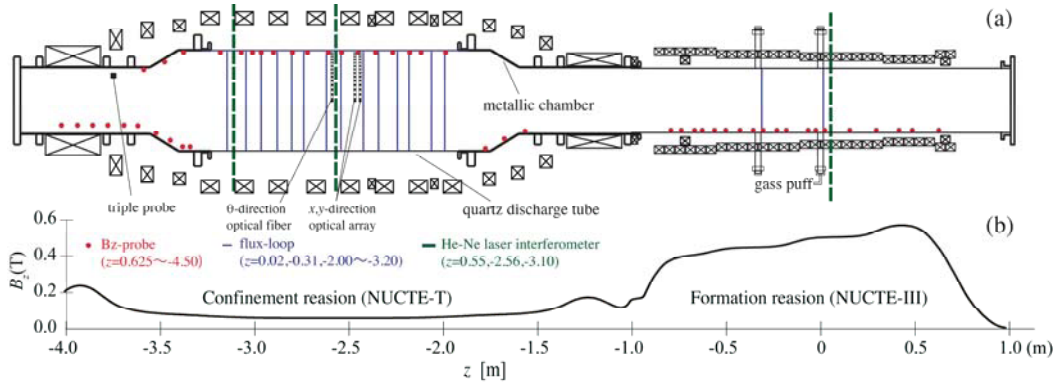


Fig. 1 Schematic view of (a) NUCTE-III/T and (b) the axial profile of a guide magnetic field.

Table 1 Typical plasma parameters of NUCTE-III/T.

Plasma parameters	v_z [km] ¹⁾	$r_{\Delta\phi}$ [m]	$l_{\Delta\phi}$ [m]	V_p [m ³]	ϕ_p [mWb]	B_z [T]	T_{total} [eV]	T_i [eV]	n_e [10 ²¹ m ⁻³]	N [10 ¹⁹]
Formation region	-80	0.05	0.6	0.01		0.58	300	160	3.0	
Confinement region	1 st pass	-150	0.09	1.9	0.04	0.7	0.065	55	0.3	0.6
	2 nd pass	90	0.09	1.8	0.03	0.5	0.065	90	0.2	0.5
	3 rd pass	-50	0.07	1.8	0.02	0.3	0.064	50	0.2	0.4

1) Negative sign denotes the direction of $-z$.

The confinement region consists of a quartz discharge tube of 1.4 m in length and 0.4 m in diameter, as a center confinement region, and two tapered stainless-steel chambers with an averaged skin time of 1.5 ms. The confinement coil consists of eight equally spaced coil elements, 0.3 m in radius and 0.1 m in width. The coil spool has a toroidal cut with a width of 0.05 m, at $y = 0.3$ m and $x = 0$. When the FRC is injected into the confinement region, an inductive current is induced on the metallic chamber.

The calculated profile of a guide field on the device axis is shown in Fig. 1 (b). The field strength of the confinement region is about 63 mT, and the mirror ratio of upstream and downstream mirrors is 2 to 3, respectively.

The axial motion of FRC plasma is monitored by an excluded flux method [5]. The arrangement of the magnetic probe array and flux loops is shown in Fig. 1 (a). An optical diagnostics system is also employed, to monitor the global behavior of the FRC. It consists of 75 collimators, and each channel has a 10 mm of resolution on the device axis [6]. An interference band-pass filter ($\lambda = 550 \pm 5$ nm) is employed to avoid impurity line spectra. Therefore, measured emission is purely bremsstrahlung. The collimators are flexibly arranged into vertical, horizontal and azimuthal directions. A first set of 34 collimators are arranged parallel to the y -axis and the x -axis, spaced at intervals of 2 cm at $z = -2.46$ and -2.43 m, respectively. A second set of six collimators are azimuthally arranged at every 18° on the plane of $z = -2.58$ m, to measure the toroidal mode of deformation. A third set of 17 collimators are axially arranged from $z = -3.19$ to 0.44 m.

In Table 1, typical plasma parameters are listed, in-

cluding translation velocity v_z , the maximum excluded flux radius $r_{\Delta\phi}$, plasma length $l_{\Delta\phi}$, plasma volume V_p , poloidal flux ϕ_p , external field B_z , plasma temperature T_{total} , ion temperature T_i , electron density n_e , and total inventory N .

3. Estimation of the Induced Current and Separatrix Shape

Typically, the separatrix radius and its profile of a FRC are estimated by an excluded flux method [5]. However it has been indicated that the resolution of this method is not enough to draw the curved separatrix profile even in the static FRTP FRC plasma [7]. Therefore, the separatrix shape of translated FRC plasma is estimated based on the effect of the induced current on the metallic boundary, by using the simple ring currents model. The conducting boundary and FRC are simulated as a set of ring currents. Here, the parameter of the ring currents (positions and strengths) is determined for the experimentally observed magnetic field density and flux. Then, the magnetic flux surface of the FRC plasma is estimated, including the effects of the metallic chamber.

To simplify the analysis, 10 ring currents are set at equal intervals within the separatrix, estimated by the excluded flux method [5]. Each radius of the current rings is defined as $r_{\Delta\phi}/\sqrt{2}$ with the measured separatrix radius $r_{\Delta\phi}$. The ring currents of the conducting wall are arranged on the inner surface of the wall. Each coil spool is simulated as one ring current, and the tapered chamber is a set of three ring currents.

Vector \mathbf{x} and \mathbf{b} denote n -elements unknown (the cur-

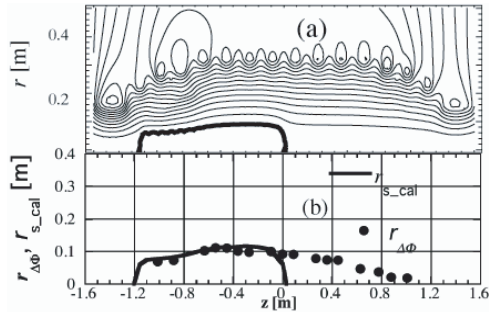


Fig. 2 Profile of FRC without toroidal cut at 30 μ s. (a) Poloidal flux surface and reconstructed separatrix $r_{s,cal}$ (thick line) and (b) $r_{s,cal}$ with experimentally observed separatrix radius $r_{\Delta\phi}$.

rent values of modeled ring currents) vector, and the measured datum (magnetic field strength and flux) of m -elements vector, respectively, which are related thus:

$$b_p - b_v = Fx_c, \quad (1)$$

where F is a coefficient $n \times m$ matrix for magnetic field and flux, and the subscripts p, v and c denote plasma, vacuum and model current values, respectively. The least-squares approach of minimizing $|b_p - b_v - Fx_c|^2$ for x_c is applied. Then the solution of the equation (1) becomes

$$x_c = (F^t F)^{-1} F^t (b_p - b_v). \quad (2)$$

The contour plot of a poloidal flux ϕ_p estimated by this model is shown in Fig. 2 (a). The calculated separatrix profile shape ($r_{s,cal}$) is defined as a contour line of $\phi_p = 0$ which is compared with the separatrix profile $r_{\Delta\phi}(z)$ estimated by the excluded flux method in Fig. 2 (b). The estimated separatrix shape of the front side is similar to the one estimated by the conventional excluded flux method. However, the back-side is different from the shape estimated by the conventional method.

The estimated inductive current at the up and downstream metallic wall, and coil spool, are -5 , 14 , and 20 kA, respectively. Then, a total plasma current of -540 kA can be estimated. In Table 2, induced currents from 20 to 45 μ s are summarized. When the FRC is injected into the metallic chamber, the inductive current on the downstream chamber wall increases from approximately -4 to 20 kA. Then, it decreases to about 2.5 kA when the plasma is reflected out from the metallic chamber region.

The Lorentz force acting on the FRC plasma from the coil spool can be estimated as approximately 50 N at 30 μ s, and is 10% of the accelerating force of about 480 N by the gradient of the magnetic guide field. In this calculation, FRC is modeled as an assembly of magnetic dipole moments. The estimation suggests that the translation velocity can be increased by reducing the induced currents. Therefore, in this series of experiments, the coil spool with a toroidal cut is used to verify this effect.

Table 2 Estimated inductive and plasma currents.

Time [μ s]	20	25	30	35	40	45
Axial plasma position [m]	-2.2	-2.5	-3.2	-3.25	-3.2	-2.5
Upstream chamber [kA]	7.9	-2.2	-5	-4.7	-7.6	-7.2
Downstream chamber [kA]	-4.3	0.9	20	22	15	2.5
Coil spool [kA]	18	22	14	14	17	21
Plasma current [kA]	-320	-500	-540	-450	-540	-320

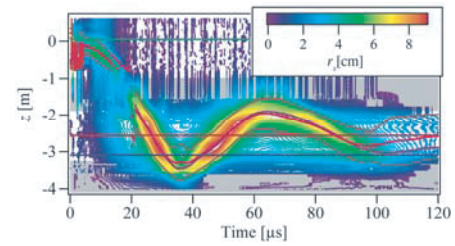


Fig. 3 Time evolution of separatrix profile. The contour denotes profile of $r_{\Delta\phi}$, and solid line shows axial positions of the x -points, and midplane of FRC.

4. Experimental Results

The induced current may stabilize MHD instabilities and reduce the wall-plasma interactions. However, in this work, translation experiments of FRC have been performed with toroidal cut on the coil spools focusing on its deceleration effect on the translation.

The time evolution of the FRC profile in the confinement region is shown in Fig. 3. The contour and the solid lines indicate the time evolution of $r_{\Delta\phi}$, axial positions of the x -points, and the midplane of the FRC, respectively. The FRC plasma is formed by a FRTP method at $t = 8$ μ s, and ejected into the confinement region with a translation velocity of 80 km/s. At the first pass, the FRC rapidly decompressed to a volume four times larger than that in the formation region. The plasma accelerated to 150 km/s and was then reflected at the downstream mirror with a mirror ratio of about three. This peak velocity is 50 km/s faster than the previous case without toroidal cut. At this point, the translated velocity decreased to 90 km/s. After three reflections, the plasma entered a static phase.

The time evolution of a line integrated electron density N_L , a line integrated intensity of bremsstrahlung I_A and $r_{\Delta\phi}$ in the translation process, is shown in Fig. 4. The magnetic structure, density, and bremsstrahlung, indicate two regions, core (closed field line one) and edge (open field line one) respectively, forming the bulk of the FRC. The ‘mass’ of magnetic structure moves faster than the electron density.

The time difference between the peaks of N_L and $r_{\Delta\phi}$ indicated by dashed line in Fig. 4 is about 2 μ s at each pass.

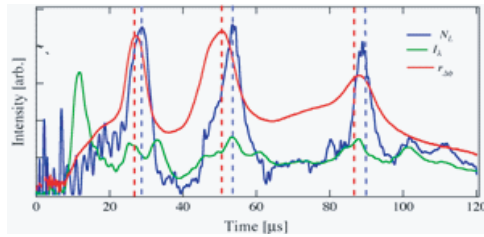


Fig. 4 Time evolution of $r_{A\phi}$ (red), N_L (blue) and I_λ (green) at $z = -2.56$ m.

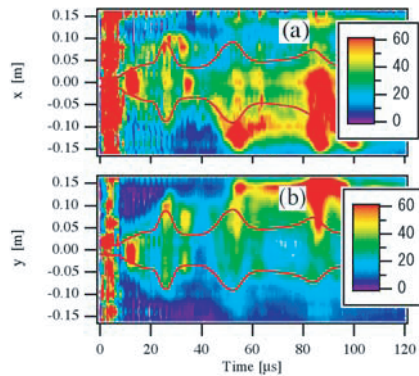


Fig. 5 (a) x -profile and (b) y -profile of line integrated intensity I_λ . The solid line denotes the time evolution of $r_{A\phi}$.

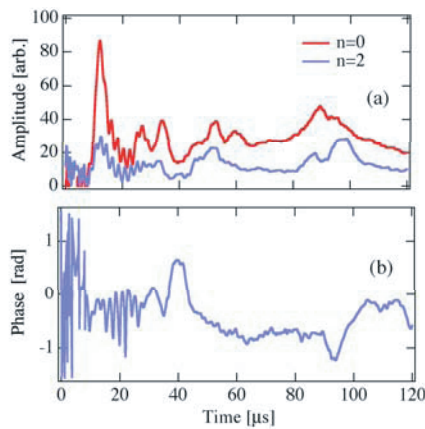


Fig. 6 Time evolution of (a) amplitudes of toroidal mode (mode number $n = 0$ and 2) and (b) phase of line integrated I_λ .

The intensity I_λ increases in the vicinity of the core of density mass N_L during the fast pass, and the structure maintains its integrity until the onset of rotational instability ($\sim 100 \mu\text{s}$), as shown in Fig. 6.

To verify the effect of a toroidal cut on the global behavior of translated FRC plasma, the time evolution of the profile of I_λ on the x (horizontal) - y (vertical) plane (mid-plane) has been measured (Fig. 5). The bremsstrahlung emissivity is proportional to the squared electron density and effective charge number for the uniform temperature

profile [8]. Therefore, non-uniformity in the I_λ profile reflects a shifted plasma density profile. In Fig. 5 (a), the peak shifted in the negative direction in the 2nd pass, and then moved back to the center in the 3rd pass. Figure 5 (b) indicates that the plasma column shifted in the positive direction of the y -axis (i.e., the direction of the toroidal cut) during the translation process.

The amplitude and phase of $n = 2$ deformation, estimated by mode analysis of the azimuthal profile of I_λ , are shown in Fig. 6. Until the 3rd major peak ($\sim 95 \mu\text{s}$), the phase does not rotate and amplitude does not increase. Therefore, this 3rd peak may be seen as an onset of rotational instability which usually terminates FRC configuration.

5. Summary

The effects of the conducting boundary on the FRC translation process have been investigated using metallic coil spools with a toroidal cut. The translation velocity increases up to 150 km/s and is 1.5 times faster than the case without a toroidal cut. This indicates that the deceleration force by the inductive current was suppressed by the toroidal cut on the spool.

However, in the case of the translation with a toroidal cut, a global shift ($n = 1$) motion would be triggered by the asymmetry of the wall boundary. A control method for this shift motion should be considered in any search for more stable translation [9].

Acknowledgements

The support from Fusion Plasma Laboratory, Nihon University, is gratefully acknowledged. This work was partially supported by Grant-in-Aid for Scientific Research (KAKENHI) 21740403 and 19560829, Nihon University Research Grant 2009, and Nihon University Strategic Projects for Academic Research.

- [1] H.Y. Guo, A.L. Hoffman, L.C. Steinhauer and K.E. Miller, Phys. Rev. Lett. **95**, 175001 (2005).
- [2] M.W. Binderbauer, H.Y. Guo, M. Tuszewski *et al.*, Phys. Rev. Lett. **105**, 045003 (2010).
- [3] Y. Matsuzawa, T. Asai, Ts. Takahashi and To. Takahashi, Phys. Plasmas **15**, 082504 (2008).
- [4] T. Asai, Y. Matsuzawa, N. Yamamoto *et al.*, J. Plasma Fusion Res. Series **8**, 1058 (2009).
- [5] M. Tuszewski and W.T. Armstrong, Rev. Sci. Instrum. **54**, 1611 (1983).
- [6] Ts. Takahashi, H. Gota, T. Fujino *et al.*, Rev. Sci. Instrum. **75**, 5205 (2004).
- [7] H. Gota, T. Akiyama, K. Fujimoto *et al.*, Rev. Sci. Instrum. **74**, 2318 (2003).
- [8] T. Asai, T. Takahashi, T. Kiguchi *et al.*, Phys. Plasmas **13**, 072508 (2006).
- [9] K. Fujimoto, A. Hoshikawa, S. Ohmura, T. Takahashi, Y. Nogi and Y. Ohkuma, Phys. Plasmas **9**, 171 (2002).